Proceedings of HT-FED04
2004 ASME Heat Transfer/Fluids Engineering Summer Conference
July 11-15, 2004, Charlotte, North Carolina USA

HT-FED04-56814

The Effect of Reynolds Number on the Ventilation Efficiency in a Wind Tunnel

Jun Li, Ibrahim Yavuz, Ismail B. Celik
Mechanical and Aerospace Engineering Department
West Virginia University, Morgantown WV 26506-6106

Steven E. Guffey
Industrial and Management Systems Engineering Department
West Virginia University, Morgantown, WV 26506

ABSTRACT

The present work is concerned with the effect of the ventilation intensity on the worker exposure in a tunnel when the worker is facing the downstream direction and a gaseous contaminant is released in an arm length of his reach. A three-dimensional model of a manikin which was used in the experiments was created in order to study the effect of the mean inlet velocity which can be characterized by the Reynolds number based on the equivalent diameter of the head of the manikin. For this study, turbulent flow was assumed to enter the ventilation tunnel and exit at the other end from an exhaust duct. The scalar transport method was employed to determine the ethanol vapor concentration field. The results with the low_Re RNG turbulence model are compared to the ones with the RNG turbulence model. The results with the RNG k-ε turbulence model seem to agree better with the experimental data at higher Reynolds numbers. At lower Reynolds numbers there are significant differences between experiments and predictions.

KEYWORDS: RANS, RNG turbulence model, exposure assessment, Reynolds Number

NOMENCLATURE

C	mean concentration
S_c	scalar source term
ρ	density
Re	Reynolds number (based on head dimension)
σ_c	laminar Schmidt number
$\sigma_{c,t}$	turbulent Schmidt number
x_i	Cartesian coordinate in tensor notation
μ	fluid dynamic viscosity
μ_t	turbulent viscosity
μ_{eff}	effective viscosity
ν	kinematical viscosity
ν_t	turbulent kinematical viscosity
t	time
k	turbulent kinetic energy
ε	turbulent dissipation rate
$\overline{U}$	averaged velocity
I	turbulent intensity
l	turbulence length scale

INTRODUCTION

Wind tunnels are widely used to study human exposures to airborne contaminants because they allow investigators to control airflow conditions. Usually, the wind speed in a ventilation tunnel is 100-150 fpm, which is comparable with the face velocities of local ventilation hoods. However, for full-scale studies, the large airflow rate due to the large cross section requires relatively high energy consumption. A thorough numerical analysis on the effect of Reynolds number on the exposure level may help to optimize the running conditions of the wind tunnel and alleviate the economic limitations to some extent. In the current study, the flow around a worker is investigated for the important case where the air flows from the back of the worker towards the direction he is facing. This flow creates, among other things, a recirculation region around the head, and it forms a wake flow with complex dynamics. The Reynolds number used in this paper is based on the head dimension, as the wake formed behind the head plays a significant role in the worker exposure levels.

Neither Direct Numerical Simulation (DNS) nor Large Eddy Simulation (LES) is practical to solve this problem because of the complex geometry of the human body. Different Reynolds-averaged Navier-Stokes (RANS) turbulence models have been used previously in predicting the flow field around a human body (Hyun and Kleinstreuer, 2001; Flynn and Sills, 2001; Longest et al., 2000; Li et al., 2003). The RNG

turbulence model has shown better capability in predicting the turbulence quantities consistent with the Reynolds Stress Model results (Li et al., 2003). In the current study, it is interesting to compare the low_Re RNG turbulence model to the RNG turbulence model, which is not well documented in the literature. In addition, the laminar flow is also simulated for 690<Re<3450, since we don't know if the flow is turbulent or not in this Reynolds number range.

The objective of this study is to evaluate the performance of the low_Re RNG turbulence model compared to the RNG turbulence model, in the assessment of the exposure levels of a worker in front of a gaseous contaminant, and to investigate the effect of the velocity of the ventilation intensity on the exposure levels.

COMPUTATIONAL DETAILS

The simulations have been performed using the Fluent CFD software package (Fluent, Inc., Lebanon, NH). The geometrical configuration of the flow domain is shown in Figure 1, consisting of the wind tunnel (4.6m width × 2.6m height × 11m length), and a manikin (1.69m height). The human body faces downstream of the isothermal flow. The fluid medium is air.

Turbulence Model

The RNG based turbulence model is derived from the instantaneous Navier-Stokes equations, using the Renormalization Group method (RNG). The details on how to derive the RNG turbulence model may be found in Yakhot and Orszag (1986). The scale elimination procedure in RNG theory results in a differential equation for turbulent viscosity:

$$d\left(\frac{\rho^2 k}{\sqrt{\varepsilon k}}\right) = 1.72\frac{\hat{\nu}}{\sqrt{\hat{\nu}^3 - 1 + C_\nu}}d\hat{\nu} \tag{1}$$

where $\hat{\nu} = \mu_{eff}/\mu$, $C_\nu \approx 100$, and $\mu_{eff} = \mu_t + \mu$.

In the high Re limit, μ_t tends to

$$\mu_t = \rho C_\mu \frac{k^2}{\varepsilon} \tag{2}$$

with $C_\mu = 0.0845$, derived using the RNG theory. It has the same form as the standard k-ε turbulence model, except $C_\mu = 0.09$ is used by the latter. The model parameters in the ε equation are also different from those for the standard k-ε model. In this paper, the low_Re RNG turbulence model represents the model using differential equation (1) and the RNG turbulence model is represented by equation (2). Besides the difference in the model parameters, another major difference between RNG and standard k-ε is that there is an additional term in the ε equation for the RNG turbulence model, which accounts for the effect of the rapid strain. The RNG model is known to be more responsive to the effects of rapid strain and streamlines curvature than the standard k-ε model, which explains the better performance of the RNG model for certain classes of flows.

Scalar Transport

If a species (ethanol in the present study) is added to the system, the mean concentration can be calculated by making use of the following transport equation:

$$\frac{\partial C}{\partial t} + \frac{\partial}{\partial x_i}\left[u_i C - (\frac{\nu}{\sigma_c} + \frac{\nu_t}{\sigma_{c,t}})\frac{\partial C}{\partial x_i}\right] = S_C \tag{3}$$

Here, S_C is the source term. σ_c is the laminar Schmidt number and $\sigma_{c,t}$ is the turbulent Schmidt number. σ_c=1.32 and $\sigma_{c,t}$=0.7 are used in this paper. (Mills, 1995)

A source pan (ϕ=0.23 m) as shown in Figure 2 is used to release the mixture of nitrogen and ethanol vapor from 90 small holes (5 mm) in the experimental study. The source pan is 1.04m above the ground at the manikin's waist height and 0.25m downstream of the manikin's torso. The mass flow rates of nitrogen and ethanol vapor are 1.98e-5 kg/s and 9.34e-7 kg/s, respectively. The mass average velocity of the released mixture is 0.0026 m/s in the vertical direction. The nitrogen is treated as air in the numerical study since this approximation greatly simplifies the calculation without loss of accuracy (By numerical experimentation it has been verified that the concentration at the breathing zone is not affected by the presence of the nitrogen). Source terms including mass, momentum in the vertical direction, as well as turbulence quantities such as k and ε are added to the corresponding equations in the source pan region (the green region in Figure 1). The turbulence quantities are calculated from

$$k = \frac{3}{2}(\bar{U}I)^2 \tag{4}$$

$$\varepsilon = C_\mu \frac{k^{3/2}}{l} \tag{5}$$

where $\bar{U}$ is the average velocity of the mixture, I is the turbulent intensity which is assumed 30% to be in the present study, and l is the turbulence length scale (which equals the diameter of the hole).

A source term representing the ethanol vapor is also added to the scalar transport equation in the same region. In addition, a thin volume underneath the releasing region is set as an impermeable zone to simulate the bottom surface of the source pan.

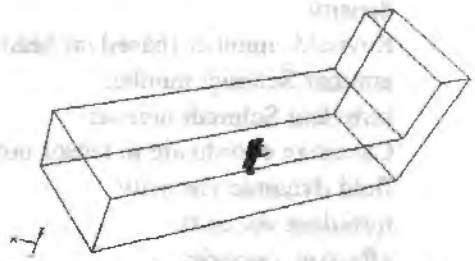

Figure 1 Schematic view of the computational domain

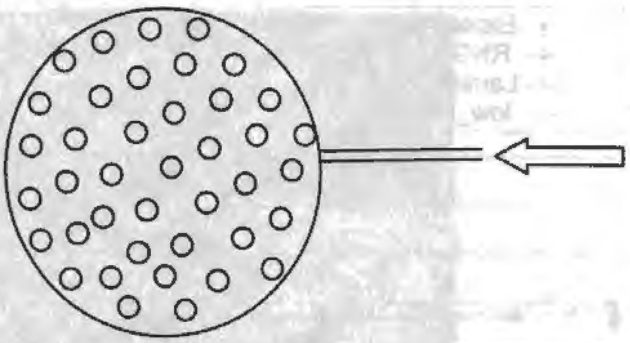

Figure 2 Top view of the source pan

Boundary Conditions

Constant velocity inlet and pressure outlet boundary conditions were used. The inlet velocity was varied in the range 0.051-0.762 m/sec (10-150 fpm) with a turbulence intensity of 10%, values representative of typical working environments (Baldwin and Maynard, 1998). The characteristic turbulent length scale was chosen to be 0.01 m, which represents the turbulence generating honeycomb size at the inlet of the tunnel. At solid surfaces the usual non-slip and impermeability conditions are applied. The standard wall function is used for the calculation with turbulence models.

Other Considerations

The mesh at the center plane is illustrated in Figure 3. The grid around the manikin is much finer. The smallest tetrahedral grid size on the manikin surface is around 0.005 m. The hexahedral mesh is used in other regions to make the computation cost affordable. In total there are around 1,100,000 cells. Using this grid, a fairly grid independent solution could be obtained (Li et al., 2003).

The SIMPLE scheme is used to solve the pressure-velocity coupling. QUICK Scheme is applied to calculate the momentum and scalar transport equations. Second order upwind scheme is used for turbulence quantities.

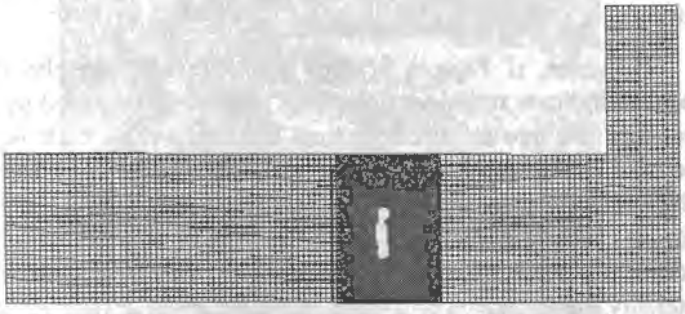

Figure 3 The computational mesh in the center plane

RESULTS AND DISCUSSION

Before the effect of Re is analyzed, some consideration should be addressed on the unsteadiness of the flow. It can be seen from Figure 4 that the concentration at the breathing zone (In this study, the breathing zone is represented by a point 1 cm downstream of the mouth) predicted with low_Re RNG varies significantly with iteration (pseudo time marching). Without appropriate averaging, the instantaneous concentrations calculated with low_Re RNG can't be compared with experimental data. It should be noted that the measurements were obtained on a relatively long time (15 minutes) sampling, hence represent ensemble averaged values. Details on the experiment are described in a paper submitted elsewhere (Guffey, 2004). To obtain reasonable mean concentrations, we need at least 1000 iterations for low_Re RNG, but 500 iterations would be enough for RNG. Simulations with low_Re RNG demand more computational cost than that with RNG. The mean data shown in Figure 5 are averaged values of 1000 iterations for low_Re RNG and laminar flow, and 500 iterations for RNG. A detailed unsteady simulation could provide the typical frequencies of the flow, which could clarify if 15-minute sampling time is sufficient for the contaminant sampling.

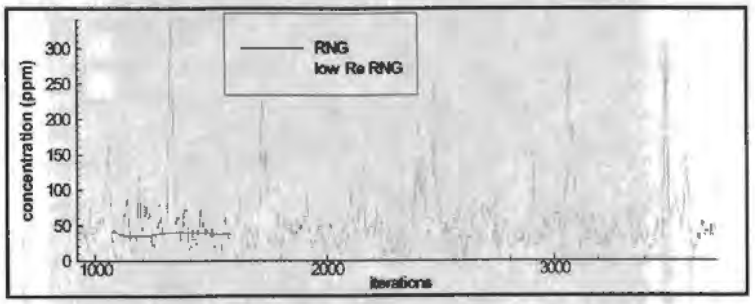

Figure 4 Concentration at the breathing zone vs. iterations at an inlet velocity of 30 fpm

Figure 5 presents the comparison of the numerical and experimental results of the concentration at the breathing zone. When the inlet velocity is greater than 90 fpm (0.46 m/s), the numerical results with both low_Re RNG and RNG agree well with the experimental ones. The concentration at the breathing zone changed very little in this Re range. When the inlet velocity is in the range of 30-90 fpm (0.15-0.46 m/s), the calculated results with the RNG model still have good agreement with the experiment. When the inlet velocity is below 30 fpm (0.15 m/s), the simulations lead to much higher exposure levels than the experiments. Overall, low_Re RNG and RNG give 20-30% different results at low Re (Re<3000 in this study). The results predicted with low_Re RNG at low Re are much higher than the experimental results and more like the ones calculated with laminar flow.

Figure 6 shows that the coefficient of variation (standard deviation divided by the mean) of the concentrations with low_Re RNG are much higher than the ones with RNG and more like the results obtained from laminar flow simulations. Averaging over iterations is necessary for calculating the mean quantities with low_Re RNG, even at Re = 10000.

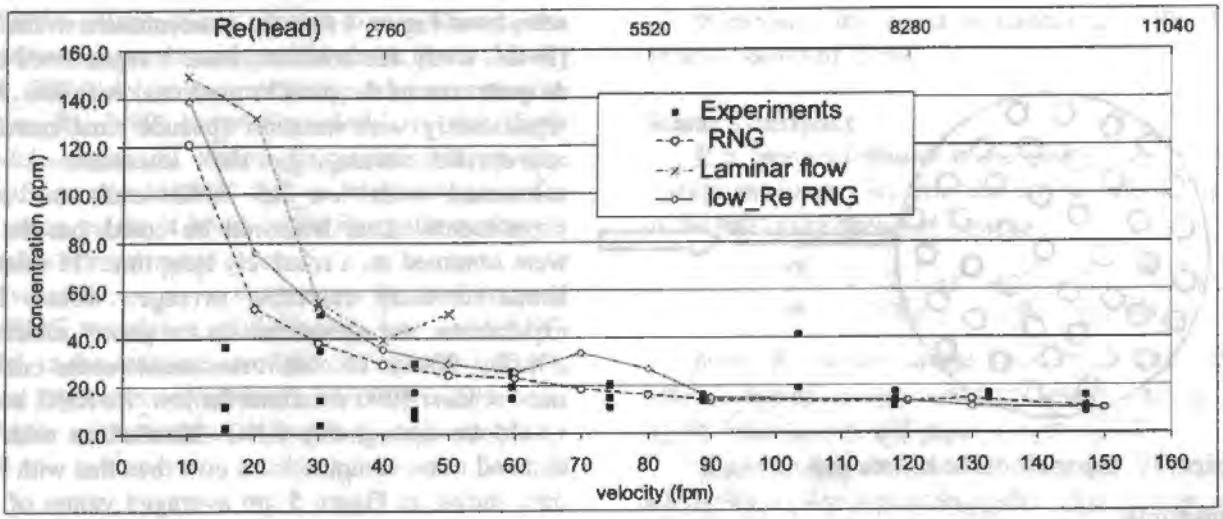

Figure 5 Comparison of the numerical and experimental results of the concentration at the breathing zone

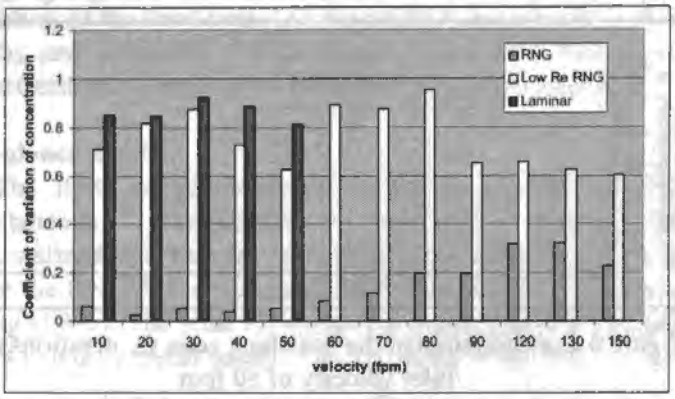

Figure 6 The coefficient of variation of the concentrations at different inlet velocities with laminar flow and two turbulence models

Figure 7 shows the instantaneous concentration contours and the pathlines in the center plane at a certain iteration moment. It can be seen that the pathlines with low_Re RNG shows more recirculation zones. From Figure 7(b), it is clear that there are two large recirculation zones in the center plane. The upper one is formed due to the separation of the flow from the head, and it can bring the gaseous contaminants to the breathing zone. The lower one is created by the flow past the legs and this may affect the size of the high concentration region. Comparing 7 (d) with 7(b), we can see that the upper recirculation zone at inlet velocity of 90 fpm (0.46m/s) has similar shape with the one at 30 fpm (0.15 m/s). However, the size of the upper recirculation zone at higher Re becomes bigger, which seems to reduce the size of the lower recirculation region. As a result the high concentration region is concentrated to a much smaller region.

The concentration contours and the pathlines at another iteration shown in Figure 8(a) illustrate how different the flow field and the concentration field could be at different instants. When the low_Re RNG turbulence model is used, a highly unsteady flow is predicted. At the shown pseudo time, the flow directly transports the contaminant to the breathing zone, which should correspond to a peak in Figure 2. Figure 8(b) shows how the flow separates from the head and forms a recirculation region. A similar behavior is also seen in Figure 9(a), which shows the conducted Particle Image Velocimetry (PIV) measurements.

The turbulent viscosity contours with RNG are shown in Figure 10. The high turbulent viscosity region indicates the separated shear layer flow there. When the Reynolds number increases from 2070 to 6210, the turbulent viscosity also increases, which indicates a higher turbulence. Whereas, the calculations with the low_Re RNG model predicted an almost laminar flow field for both Reynolds numbers, i.e. a very low turbulent viscosity. This indicates that the low_Re RNG model predicts a flow field which is more like a laminar flow around a sphere. The flow over a sphere remains laminar up to a Re of ~10^5. Nevertheless, the Re subject for this study is much lower than this number and may indicate that the actual flow may be laminar.

However, if Figures 9(a&b) are observed closely, they seem to indicate turbulent flow. This could be explained by the fact that the free stream flow may be turbulent, which is not the case in the simulations. Then, it could be reasoned that the RNG model is causing a turbulent flow field, which in turn exhibit better agreement in comparison to experiments. Additional experiments are needed to measure the turbulence intensity and length scale in the free stream and to clarify, if the free stream flow is indeed turbulent.

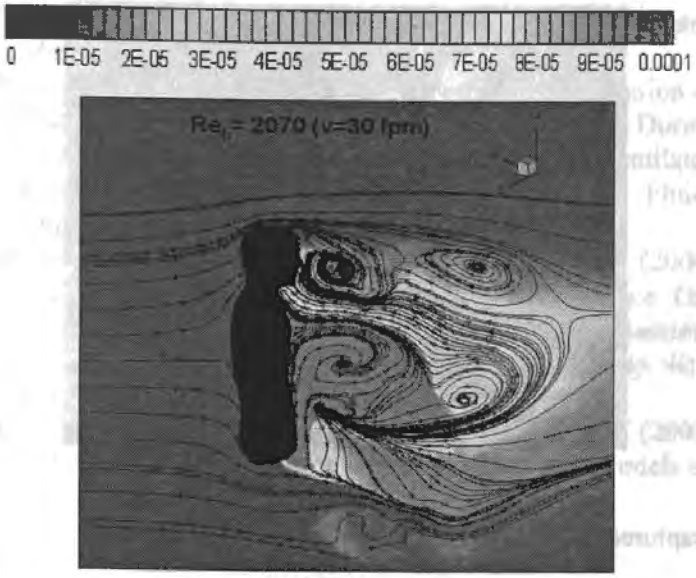

a) low_Re RNG

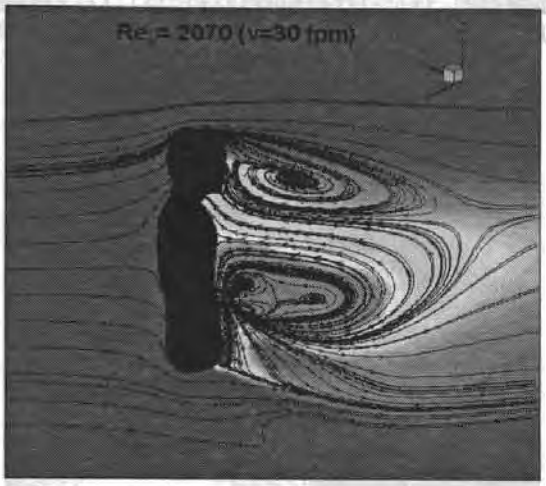

b) RNG

c) low_Re RNG

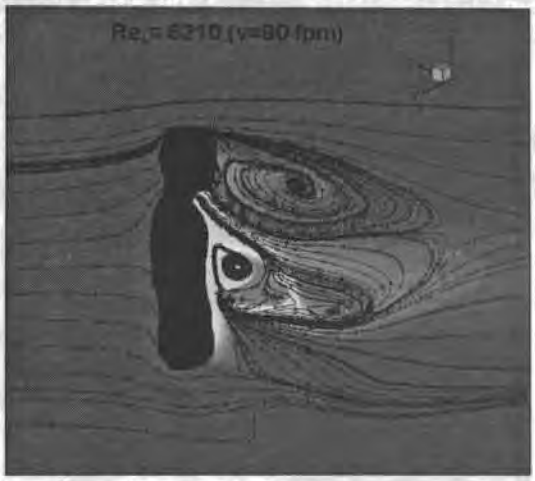

d) RNG

Figure 7 Concentration contours and pathlines in the center plane

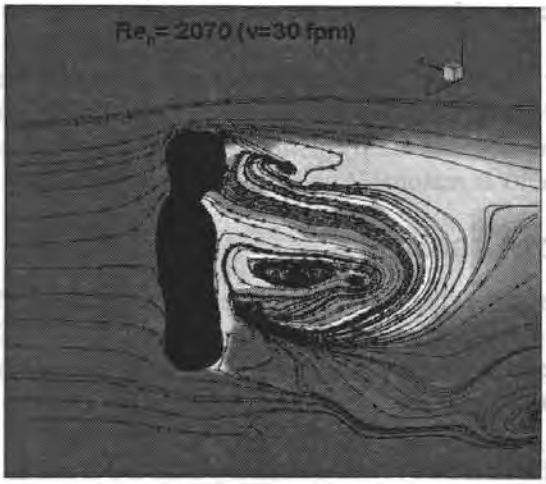

a) low_Re RNG

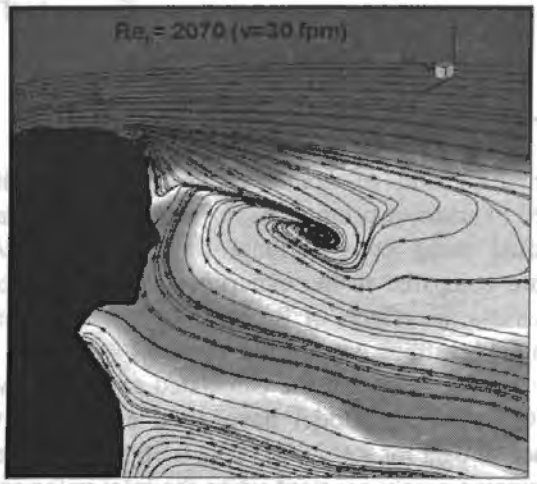

b) low_Re RNG (Close up around the head)

Figure 8 Concentration contours and pathlines in the center plane at another iteration moment different from the one in Figure 7

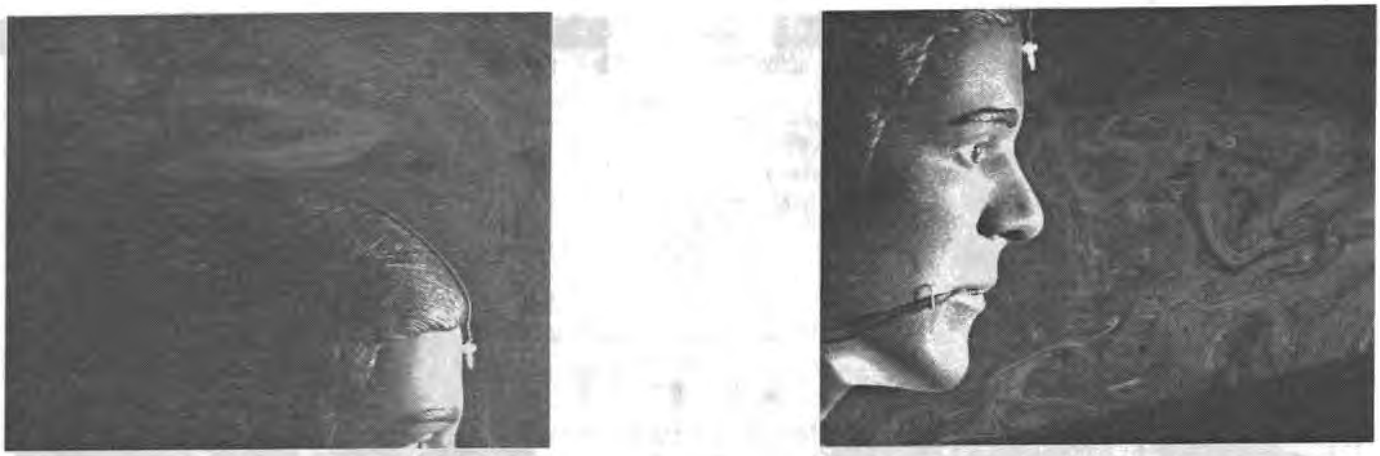

a) V(inlet) = 47 fpm

b) V(inlet) = 97 fpm

Figure 9 Instantaneous smoke test images captured by PIV (Guffey, 2004)

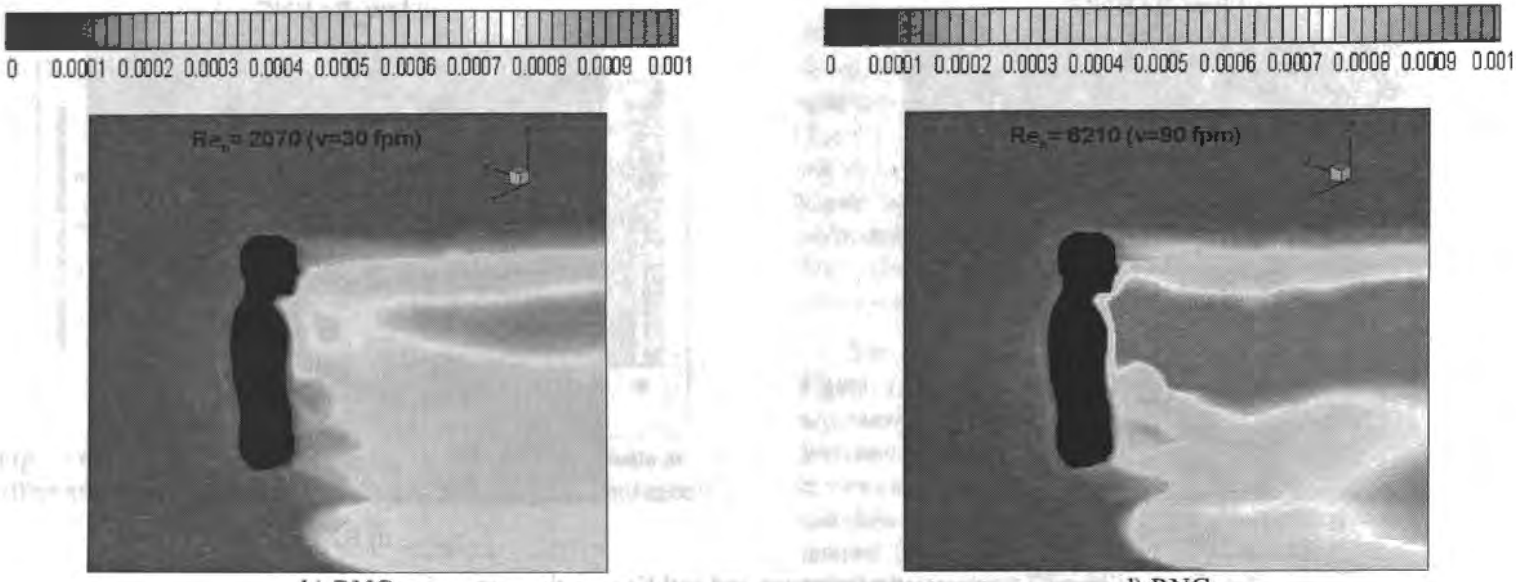

b) RNG

d) RNG

Figure 11 Turbulent viscosity in the center plane

CONCLUSION

The dispersion of contaminants in the vicinity of a simulated human working in a wind tunnel has been investigated using computational fluid dynamics. And the results are compared to the experimental data. The objective was to assess the effects of Re on the predicted contaminant levels in the breathing zone of the worker.

The results show that the calculated exposure levels with the RNG turbulence model have good agreement with the experimental data for Re>2000 (U_{inlet} > 30 fpm). The exposure levels remains nearly constant when the inlet velocity exceeds 90 fpm (0.46 m/s). However, following the above discussion, more experimental and numerical data is needed to support this conclusion.

The unsteady flow features should be investigated thoroughly. This would reveal more realistic flow characteristics and clarify if the sampling period used in the experiments is reasonable under these flow conditions.

ACKNOWLEDGMENTS

This work has been performed under a U.S. National Institute for Occupational Safety and Health (NIOSH) project sponsored by Centers for Disease Control (CDC) under the grant R01 OH07587-01.

REFERENCES

Hyun, S. and Kleinstreuer, S. (2001) "Numerical Simulation of Mixed Convection Heat and Mass Transfer in a Human

Inhalation Test Chamber" International Journal of Heat and Mass Transfer Vol. 44, pp.2247-2260

Flynn, M.R. and Sills, E.D. (2001) "Numerical Simulation of Human Exposure to Aerosols Generated During Compressed Air Spray-Painting in Cross-Flow Ventilated Booths", Transactions of ASME, Journal of Fluids Engineering Vol. 123, pp.64-70

Longest, P.W., Kleinstreuer, C. and Kinsey, J.S. (2000) "Turbulent Three-dimensional Air Flow and Trace Gas Distribution in an Inhalation Test Chamber", Transactions of ASME, Journal of Fluids Engineering Vol. 122 pp. 403-411

Li, J., Yavuz, I., Celik, I.B., Guffey, S.E. and Bird, A. (2003) "The Effect of Turbulence and Scalar Transport Models on Prediction of Worker Exposure to Aerosols" Proceedings of FEDSM'03, 4TH ASME_JSME Joint Fluids Engineering Conference, Honolulu, Hawaii, USA, July 6–11, 2003

Guffey, S.E. (2004) "Private Communication" Industrial and Management Systems Engineering Department, West Virginia University, Morgantown, WV 26506

Baldwin, P.E.J. and Maynard, A.D. (1998) "A Survey of Wind Speeds in Indoor Workplaces" Ann. Occup. Hyg., Vol. 42, No. 5, pp. 303-313.

Mills, A.F. (1995) "Basic Heat and Mass Transfer" Richard d Irwin, 1995

Yakhot V. and Orszag, S.A., "Renormalization group analysis of turbulence", J.Sci.Comput., Vol.1, p3, (1986).